Zeolite Crystallization

DOI: 10.1002/anie.200802823

Cubes of Zeolite A with an Amorphous Core**

*Jianfeng Yao, Dan Li, Xinyi Zhang, Chun-Hua Kong, Wenbo Yue, Wuzong Zhou, and Huanting Wang**

The syntheses of zeolites involve very complex nucleation and growth processes. During the past decade, significant progress has been made towards understanding zeolite crystallization mechanisms. This progress has been made possible by advanced analytical techniques, such as high-resolution transmission electron microscopy (HRTEM), small-angle X-ray scattering, and atomic force microscopy.[1–5] A number of zeolite growth mechanisms were proposed based on the respective synthesis of the zeolites. For instance, by monitoring the crystallization of silicalite-1 from silica sols in tetrapropylammonium ion (TPA) at room temperature, an oriented aggregation mechanism was proposed.[4] In the growth mechanism of zeolite A evolving from the nuclei inside the amorphous gel, the particles gradually grow into larger crystals by consuming the surrounding amorphous gels.[2] The gel was formed by using aluminosilicate solutions and tetramethylammonium hydroxide as the structure-directing agent (SDA).[2] For zeolite A formation, evidences of nucleation at the solid–liquid interface of the gel cavities were also found in sodium aluminosilicate gels without organic SDA.[3] In addition, a reversed crystal growth process from the surface to the core of nanocrystallite aggregates was observed in the crystal growth of zeolite analcime icositetrahedra.[6] These studies have undoubtedly provided new insights into zeolite crystallization processes.

As non-structure-directing agents, organic polymers have significant effects on zeolite nucleation and growth. The confinement of sodium aluminosilicate zeolite gels in thermoreversible methylcellulose hydrogels resulted in zeolite A and X nanocrystals under hydrothermal treatment.[7] Crosslinked polyacrylamide hydrogels was used to reduce SAPO-34 crystal sizes in vapor-phase transport synthesis.[8] In all these cases, the small crystal sizes is due to space confinement of the polymer hydrogel networks. Hollow sodalite spheres and zeolite A crystals were also synthesized hydrothermally in the presence of crosslinked polyacrylamide hydrogels. It was suggested that the scaffolds of polyacrylamide hydrogels were the preferential sites for zeolite nucleation, and promoted the direction of nanoparticle aggregation subsequent to the surface-to-core growth.[9] These results suggest that the roles of polymer hydrogels in zeolite synthesis are complex, and syntheses of the zeolites depend on the microstructure of the polymer hydrogels and the interaction between the polymer chains and the zeolite gels.

Herein we report the formation of cubes of zeolite A with a single crystalline shell and an amorphous core by in-situ crystallization of sodium aluminosilicate gel inside the polymer networks of uncrosslinked chitosan hydrogel. This work provides further direct evidence for the surface-to-core reversed-growth mechanism. Chitosan is a biopolymer derived from chitin that is found in a wide range of natural sources, such as crab, lobster, and shrimp shells. Chitosan, containing abundant amino and hydroxy groups, was used as the orientation-directing matrix for the synthesis of *b*-oriented TS-1 films.[10] Glutaraldehyde-crosslinked chitosan (GA-CS) hydrogels were recently used to control zeolite crystallization, and thus zeolite A and Y nanocrystals were synthesized.[11] It is noted that chitosan is only soluble in an acidic aqueous solution, and the resulting chitosan solution turns into a polymer hydrogel when an alkaline solution penetrates through the gel. Therefore, for the synthesis of core-shell cubes of zeolite A, a two-step process, involving the dispersion of silica in a chitosan acidic solution and subsequent penetration of $Na_2O/Al_2O_3/H_2O$ alkaline solution was employed to form a sodium aluminosilicate gel inside the uncrosslinked chitosan hydrogel.

XRD pattern (Figure 1a) indicates the as-synthesized sample has the structure of zeolite A. SEM image (Figure 1b) shows cube-like crystals with a particle size of 0.5–1.5 μm. This morphology with six {100} facets is typical for zeolite A, which has a cubic structure with the unit cell parameter $a =$ 2.461 nm, and space group $Fm\bar{3}c$. The characteristic polyhedron normally indicates a single crystal property of zeolite A. According to the classic crystal growth theory, crystals normally develop from nuclei and the appearance of the facets is due to the differences in their growth rate.[12–15]

TEM confirms the cube-like or rectangular morphology of the samples. Figure 2a shows a TEM image of a typical rectangular particle of zeolite A with the corresponding

[*] Dr. J. F. Yao,[+] D. Li, Dr. X. Y. Zhang, Dr. H. T. Wang
Department of Chemical Engineering
Monash University, Clayton, Victoria 3800 (Australia)
Fax: (+61) 3-9905-5686
E-mail: huanting.wang@eng.monash.edu.au
W. B. Yue, Dr. W. Z. Zhou
School of Chemistry, University of St. Andrews,
St. Andrews, Fife KY16 9ST (United Kingdom)
Dr. C. H. (Charlie) Kong
Electron Microscope Unit
University of New South Wales, Sydney, NSW 2052 (Australia)
[+] Present address:
State Key Laboratory of Materials-Oriented Chemical Engineering
and College of Chemistry and Chemical Engineering
Nanjing University of Technology, Nanjing 210009 (P.R. China)

[**] This work was supported by the Australian Research Council (Grant No.: DP0452829). H.W. thanks the Australian Research Council for the QEII Fellowship. W.Z. thanks University of St Andrews for an EaStChem studentship to W.Y.

Supporting information for this article is available on the WWW under http://dx.doi.org/10.1002/anie.200802823.

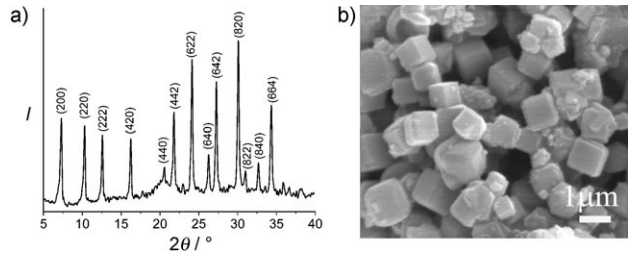

Figure 1. a) XRD pattern and b) SEM image of the as-synthesized sample.

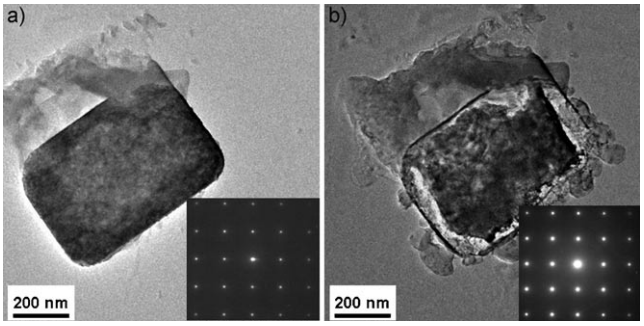

Figure 2. TEM images of a typical zeolite A particle with a cube-like morphology and the corresponding SAED patterns obtained from the entire particle. a) Original particle and b) the same particle after beam irradiation for a few minutes.

selected area electron diffraction (SAED) pattern, which is a standard single crystal diffraction pattern viewed down the [100] zone axis. Many particles were examined, and the single crystalline nature of zeolite A was observed in each case without evidence of any polycrystallinity and twin defects. However, the image contrast implies a core–shell structure, in which the core appears to be disordered. Under the electron beam of the microscope, the disordered core of the zeolite A reduced in volume and separated itself from the shell in a matter of few minutes. The shell remained intact, which clearly appeared as a rectangle with a thickness of about 7 nm (Figure 2b). The SAED pattern from the particle in Figure 2b is almost identical to the pattern in Figure 2a, which indicates that the shell structure was maintained after the irradiation and the separation of the core. No other diffraction spots were observed, indicating that the core is amorphous, rather than polycrystalline as in the case of zeolite analcime.[6] As the material is very sensitive to the beam, HRTEM images of the crystalline shell were not acquired. The low-magnification TEM images and the SAED patterns allows us to describe the zeolite A as a monocrystalline cube-like or rectangular box with an amorphous core.

The core-shell structure of the as-synthesized zeolite A was further supported by dark field TEM images of the cross-sections of the cubes prepared by focused ion beam milling (see Supporting Information, Figure SI1) and by dissolution of the core component in an acidic aqueous solution. During the latter process, 30 mL of 0.35 M acetic acid solution was added to 1 g of the zeolite A under stirring for 4 h. Most of the cubes lost their inner filling and micrometer-sized hollow cube-like structures were produced (Supporting Information, Figure SI2a). According to the XRD pattern these hollow structures were amorphous (Supporting Information, Figure SI2b). As the rate of dissolution of the amorphous core is much faster than the crystalline shell, the cube-like or rectangular outer shape was retained, although the crystallinity of the shell was lost during the acidic treatment. For comparison, zeolite A crystals were prepared without chitosan; however, the resulting particles were amorphous (Figre SI3).

To investigate the crystallization of zeolite A during the hydrothermal reaction, the products obtained during 1 to 6 h of reaction time were examined. The sample was amorphous after 1 h, whereas those obtained after 2 and 3 h had zeolite A structure. After 4 h and 6 h of hydrothermal reactions, a mixture of zeolite A and sodalite (Supporting Information, Figure SI4) was obtained. After the 0.35 M acetic acid treatment, all the crystalline samples obtained from hydrothermal synthesis of 2–6 h had a rectangular or cube-like morphology (Supporting Information, Figure SI5). These results indicate that extending hydrothermal reaction time did not lead to the crystallization of the cores of zeolite A, but resulted in the transformation of the crystal structure of the shell.

Figure 3 shows the formation of cubes of zeolite A with an amorphous core. Initially, the silica sol is dispersed in an acidified chitosan solution (Figure 3a). After addition of the alkaline solution, the chitosan molecules are deprotonated, resulting in a hydrogel with microsized three-dimensional pores (Figure 3b). The sodium aluminosilicate gel is produced inside the chitosan hydrogel network by the reaction between silica and the alkaline solution. During the hydrothermal treatment, zeolite nucleation takes place mainly on the surface of the aluminosilicate aggregates (Figure 3c). Similar to the case of zeolite analcime,[6] some crystalline islands might initially form on the surface of the aluminosilicate. These islands then join together, leading to a monocrystalline cube-like shapes by self-alignment of their crystallographic orientations (Figure 3d). Thus, it is an interesting observation that a very thin-walled crystalline cube-like or rectangular

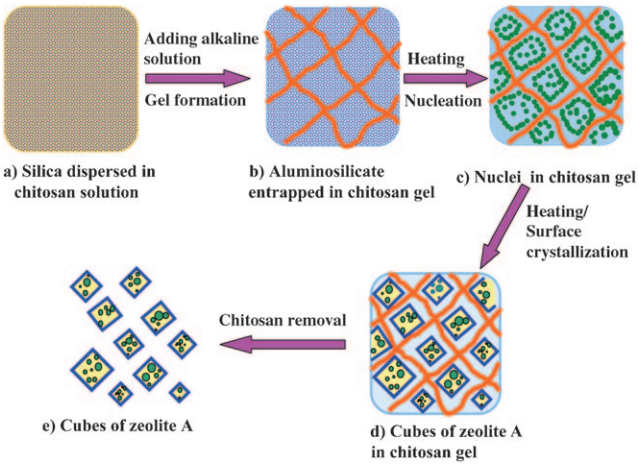

Figure 3. Representation of the formation of cubes of zeolite A, with an amorphous core (e). The rounded boxes in a)–d) are about 4 μm × 4 μm in dimension.

morphology can be developed on the surface of an amorphous cluster without any specific relationship to the crystal growth rate of the crystal planes from a nucleus in the amorphous center (Figure 3d). The driving force behind the formation of such polyhedral shells is the one that minimizes the surface energy.

It has also been observed that organic polymers have significant effects on zeolite crystallization.[7–9,11,16] The addition of water-soluble polymers in the zeolite gel could dramatically shorten the prenucleation and nucleation periods and thus accelerate the crystal growth.[16] Mathematical modeling[17,18] and experimental results[3] indicate that zeolite nucleation takes place at the interface between the solution and the gel by adsorption and rearrangement of the soluble precursors. In the synthesis described herein, the uncrosslinked chitosan hydrogel networks are highly swollen by the solution, and the interfaces between the chitosan polymer networks and zeolite aluminosilicate gel can serve as ideal nucleation sites. Such unique interfaces facilitate zeolite crystallization from the surface of the aliminosilicate gel aggregates. On the other hand, the chitosan hydrogel may also play a role in confining the aluminosilicate aggregates and thus controlling the sizes of the zeolite A cubes. During the hydrothermal treatment, the crystalline shell limits the diffusion of the solution and thus the crystallization of the cores is not able to proceed. It is worth mentioning that fully crystallized zeolite A cubes were obtained when the gel was aged overnight at room temperature before the hydrothermal treatment. The aging process most likely makes the system more uniform, in which the chitosan-facilitated zeolite nucleation becomes kinetically less pronounced. In addition, the desired network structure of chitosan hydrogels is essential for the formation of cubes of zeolite A with an amorphous core. Owing to the presence of crosslinked chitosan hydrogels, the small hydrogel pores greatly confined zeolite growth leading to zeolite nanocrystals.[11]

In summary, we have shown that cubes of zeolite A consisting of a thin crystalline shell and an amorphous core can be grown within uncrosslinked chitosan hydrogels. It is indicative that the formation of cube-like or rectangular core-shell structures involves particle aggregation and surface-to-core crystallization induced by chitosan networks. This work may provide a new model system for studying complex zeolite nucleation and growth mechanisms.

Experimental Section

Acetic acid (99%, Sigma–Aldrich; 7 g of 1M) was dissolved in deionized water (14 g) in a polypropylene bottle. Chitosan (average molecular weight 120000 g mol^{-1}, ca. 80% deacetylated, Sigma–Aldrich; 1.2 g) was dissolved in the prepared acetic acid solution under magnetic stirring for 1 h, followed by addition of the silica sol (HS-30 30 wt%, Sigma–Aldrich; 3.38 g) to the chitosan/acetic acid solution. The alkaline solution was prepared by mixing NaOH (99%, Merck; (5 g), and $NaAlO_2$ (anhydrous, Sigma–Aldrich; 2.45 g) with deionized water (20 g). The solution was stirred for 0.5–1 h until it became clear. The $Na_2O/Al_2O_3/H_2O$ alkaline solution was added to the chitosan/acetic acid solution without stirring, resulting in a sodium aluminosilicate gel entrapped inside the chitosan hydrogel. The final molar composition of chitosan/SiO_2 was 1.18:1. After hydrothermal treatment at 90°C for 3 h, the samples were washed with sufficient water and dried at 80–100°C overnight, followed by calcining the dried sample at 500°C in oxygen, or treating them with 10% hydrogen peroxide to remove chitosan.[11] In addition, samples were also synthesized at 90°C with different hydrothermal reaction times (1, 2, 4, and 6 h).

Scanning electron microscopy (SEM) images were taken with a JSM-6300F microscope (JEOL). Transmission electron microscopy (TEM) images and selected-area electron diffraction (SAED) were taken with a JEOL JEM-2011 electron microscope operated at 200 kV. X-ray diffraction (XRD) patterns were recorded on a Philips PW1140/90 diffractometer with Cu Kα radiation at a scan rate of 2° min^{-1} and a step size of 0.02°.

Received: June 14, 2008
Published online: October 2, 2008

Keywords: chitosan · crystal growth · hydrogels · polymers · zeolites

[1] C. S. Cundy, P. A. Cox, *Microporous Mesoporous Mater.* **2005**, *82*, 1–78.
[2] S. Mintova, N. H. Olson, V. Valtchev, T. Bein, *Science* **1999**, *283*, 958–960.
[3] V. P. Valtchev, K. N. Bozhilov, *J. Am. Chem. Soc.* **2005**, *127*, 16171–16177.
[4] a) T. M. Davis, T. O. Drews, H. Ramanan, C. He, J. S. Dong, H. Schnablegger, M. A. Katsoulakis, E. Kokkoli, A. V. McCormick, R. L. Penn, M. Tsapatsis, *Nat. Mater.* **2006**, *5*, 400–408; b) M. A. Snyder, M. Tsapatsis, *Angew. Chem.* **2007**, *119*, 7704–7717; *Angew. Chem. Int. Ed.* **2007**, *46*, 7560–7573.
[5] J. R. Agger, N. Pervaiz, A. K. Cheetham, M. W. Anderson, *J. Am. Chem. Soc.* **1998**, *120*, 10754–10759.
[6] X. Y. Chen, M. H. Qiao, S. H. Xie, K. N. Fan, W. Z. Zhou, H. Y. He, *J. Am. Chem. Soc.* **2007**, *129*, 13305–13312.
[7] H. T. Wang, B. A. Holmberg, Y. S. Yan, *J. Am. Chem. Soc.* **2003**, *125*, 9928–9929.
[8] J. F. Yao, H. T. Wang, S. P. Ringer, K. Y. Chan, L. X. Zhang, N. P. Xu, *Microporous Mesoporous Mater.* **2005**, *85*, 267–272.
[9] L. Han, J. F. Yao, D. Li, J. Ho, X. Y. Zhang, C. H. Kong, Z. M. Zong, X. Y. Wei, and H. T. Wang, *J. Mater. Chem.* **2008**, *18*, 3337–3341.
[10] X. D. Wang, B. Q. Zhang, X. F. Liu, Y. S. Lin, *Adv. Mater.* **2006**, *18*, 3261–3265.
[11] D. Li, Y Huang, K. R. Ratinac, S. P. Ringer, H. T. Wang, *Microporous Mesoporous Mater.* **2008**, DOI:10.1016/j.micromeso.2008.04.032.
[12] A. Bravais, *e'tudes Cristallographic*, Gauthier-Villars, Paris, **1866**.
[13] M. G. Friedel, *Bull. Soc. Fr. Mineral. Cristallogr.* **1907**, *30*, 326–455.
[14] J. D. H Donnay, D. Harker, *Am. Mineral.* **1937**, *22*, 446–467.
[15] P. Hartman, W. G. Perdok, *Acta Crystallogr.* **1955**, *8*, 49–52; P. Hartman, W. G. Perdok, *Acta Crystallogr.* **1955**, *8*, 521–524; P. Hartman, W. G. Perdok, *Acta Crystallogr.* **1955**, *8*, 525–529.
[16] G. J. Myatt, P. M. Budd, C. Price, F. Hollway, S. W. Carr, *Zeolites* **1994**, *14*, 190–197.
[17] V. Nikolakis, D. G. Vlacho, M. Tsapatsis, *Microporous Mesoporous Mater.* **1998**, *21*, 337–346.
[18] T. O. Drews, M. A. Katsoulakis, M. Tsapatsis, *J. Phys. Chem. B* **2005**, *109*, 23879–23887.

